Accelerated Publications

Conserved Gating Hinge in Ligand- and Voltage-Dependent K^+ Channels†

Elhanan Magidovich and Ofer Yifrach*

Department of Life Sciences and Zlotowski Center for Neurosciences, Ben-Gurion University of the Negev, P.O. Box 653, Beer-Sheva 84105, Israel

Received July 29, 2004; Revised Manuscript Received September 1, 2004

ABSTRACT: Ion channels open and close their pore in a process called gating. On the basis of crystal structures of two voltage-independent K^+ channels, KcsA and MthK, a conformational change for gating has been proposed whereby the inner helix bends at a glycine hinge point (gating hinge) to open the pore and straightens to close it. Here we ask if a similar gating hinge conformational change underlies the mechanics of pore opening of two eukaryotic voltage-dependent K^+ channels, *Shaker* and BK channels. In the *Shaker* channel, substitution of the gating hinge glycine with alanine and several other amino acids prevents pore opening, but the ability to open is recovered if a secondary glycine is introduced at an adjacent position. A proline at the gating hinge favors the open state of the *Shaker* channel as if by preventing inner helix straightening. In BK channels, which have two adjacent glycine residues, opening is significantly hindered in a graded manner with single and double mutations to alanine. These results suggest that K^+ channels, whether ligand- or voltage-dependent, open when the inner helix bends at a conserved glycine gating hinge.

Potassium channels are allosteric proteins that undergo conformational transitions between closed and opened states induced by changes in chemical or electrical potential (*1*−*5*). These conformational transitions underlie K^+ ion diffusion across membranes and are essential to many biological processes (*6*).

Recent X-ray crystallographic studies have provided the first pictures of structural rearrangements that probably occur when a K^+ channel opens (*7*−*10*). These pictures are based on the structures of KcsA, a K^+ channel in its closed conformation (*7, 8*), and MthK, a Ca^{2+}-activated K^+ channel in its Ca^{2+}-bound, opened conformation (*9, 10*). The main conformational change between the closed and opened pores occurs in the inner helix, which lines the ion conduction pathway on the intracellular side of the selectivity filter (Figure 1). In KcsA (the closed channel, Figure 1, left) the four inner helices (one from each subunit) are straight so that they cross over each other, forming a right-handed helical bundle that constricts the pore near its intracellular entryway. In MthK (the opened channel, Figure 1, right), the inner helices are bent so that the helical bundle comes apart, allowing a wide tunnel (∼12 Å diameter) leading from the cytoplasm to the selectivity filter.

The inner helices bend at a position that is conserved as glycine in KcsA, MthK, and many other K^+ channels (Figure 1, red highlight). Conservation of glycine at a specific location in the inner helix implies that the conformational changes underlying K^+ channel opening may be somewhat similar regardless of the opening stimulus, whether it is ligand binding or membrane voltage. In support of a conserved gating transition among K^+ channels, gating-sensitive mutations in the *Shaker* voltage-dependent K^+ channel were shown to cluster mainly at two regions (when mapped onto the KcsA structure): at the inner helix bundle crossing and near the conserved glycine (where the inner helix presumably bends) (*11*). Correlated mutation analysis using multiple-sequence alignment of the voltage-dependent K^+ channel family further demonstrates that allosteric communication network in this protein family consists mainly of residues lining these two locations (*12*). This consistency between structural, functional, and evolutionary data for different K^+ channels suggests that, in essence, pore opening mechanics in the *Shaker* voltage-dependent channel (and perhaps other K^+ channels) is similar to the opening mechanics demonstrated upon comparison of the KcsA and MthK voltage-independent channels: opening that is induced by rigid-body motion along the glycine gating hinge. Here we further test this hypothesis by studying the effects of flexibility perturbations introduced, by means of mutagenesis, at the gating hinge position. Our experiments focus on two different eukaryotic voltage-dependent K^+ channels, *Shaker* and the high-conductance (BK) calcium- and voltage-dependent K^+ channels.

EXPERIMENTAL PROCEDURES

Molecular Biology and Electrophysiology. Mutations in *Shaker*-IR (*13*) (residues 6−46 deleted) or in hslo cDNAs were introduced by the QuickChange method (Stratagene)

† This research was supported (in part) by the Israel Science Foundation (Grant 323/04 to O.Y.).

* To whom correspondence should be addressed. Telephone: ++972-8-6479172. Fax: ++972-8-6461710. E-mail: ofery@bgu.ac.il.

10.1021/bi048377v CCC: $27.50
Published on Web 10/02/2004

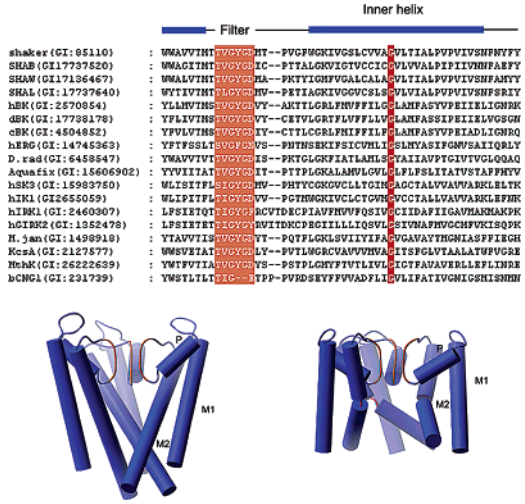

FIGURE 1: Sequence and structural analyses suggest conserved gating hinge motions upon pore opening. (A) Shown are sequences from the inner helices of various ligand and voltage-dependent K^+ channels and a CNG channel. The selectivity filter is colored orange and the gating hinge glycine red: *Shaker*, *Drosophila melanogaster* Kv 1.1 K^+ channel; SHAB, *D. melanogaster* Kv 2.1 K^+ channel; SHAW, *D. melanogaster* Kv 3.1 K^+ channel; SHAL, *D. melanogaster* Kv 4.1 K^+ channel; hBK, *H. sapiens* BK channel; dBK, *D. melanogaster* BK channel; cBK, *Caenorhabditis elegans* BK channel; hERG, *H. sapiens* eag-type K^+ channel; D.rad, *Deinococcus radiodurans* putative voltage-dependent K^+ channel; Aquafix, *Aquifex aeolicus* putative voltage-dependent K^+ channel; hSK3, *H. sapiens* small conductance K^+ channel; hIK1, *H. sapiens* intermediate conductance K^+ channel; hIRK1, *H. sapiens* inward rectifying K^+ channel; hGIRK2, *H. sapiens* G-protein-activated K^+ channel; M. Jan, *Methanococcus jannaschii* K^+ channel; KcsA, *Streptomyces lividans* K^+ channel; MthK, *Methanococcus thermautotrophicum* K^+ channel; and bCNG1, *Bos taurus* cyclic nucleotide-gated channel. GenBank accession numbers are given in parentheses. (B) Shown at the bottom are three subunits of the KcsA (left) and MthK (right) closed and open pore structures, respectively, with colors corresponding to those in panel A. M1, P, and M2 denote the outer, pore, and inner helices, respectively.

and confirmed by sequencing the entire cDNA. To evaluate channel expression in *Xenopus* oocytes, a six-histidine tag was added to the C-terminus of either wild-type or mutant K^+ channels using site-directed mutagenesis. RNA was prepared by T7 polymerase transcription and injected into *Xenopus laevis* oocytes. K^+ currents were recorded under a two-electrode voltage clamp (OC725B, Warner Instruments Corp.) 1−2 days after *Shaker* mRNA injection (~50 ng). Electrodes were drawn from borosilicate glass capillaries (World Precision Instruments) to a resistance of ~0.5 MΩ (3 M KCl). Bath solution contained 58 mM NaCl, 40 mM RbCl, 0.3 mM $CaCl_2$, 1 mM $MgCl_2$, and 5 mM HEPES (pH 7.6). Oocytes were typically held at −100 to −80 mV and were stepped to different test voltages followed by repolarization, usually to the holding voltage. The tail current amplitude was typically measured 2−4 ms after repolarization.

Macroscopic currents were recorded (Axopatch 200B, Axon Instruments) from the BK channels using inside-out patches excised from oocytes 2−4 days after mRNA injection. Electrodes were drawn from patch borosilicate glass (PG150T-10, Warner Instruments) and were polished to a resistance of 1−2 MΩ. The pipette solution contained 140 mM potassium gluconate, 20 mM KCl, 20 mM HEPES (pH 7.5), 2 mM $MgCl_2$, 1 μM $CaCl_2$, and 5 mM EGTA. The bath solution was identical to the pipette solution but contained 1 or 100 μM free $CaCl_2$ and no $MgCl_2$. Free calcium ion concentrations were set by adding the appropriate amount of $CaCl_2$ calculated using a value of 3.86×10^{-7} M for the equilibrium constant for formation of the EGTA−Ca^{2+} complex. Patches were first excised in a bath solution containing 1 μM free $CaCl_2$, and K^+ currents were recorded after gravity flow solution exchange with a bath solution containing 100 μM free $CaCl_2$. K^+ currents were elicited by various strength depolarizations from a holding potential of −100 mV followed by repolarization, typically to −60 mV. For any given patch, three data sets were acquired and averaged. Five to eight patches were measured for wild-type or mutant BK channel proteins, and the data were averaged after normalization. Analogue data from the amplifier were filtered (2−4 kHz, −3 dB) using a low-pass Bessel filter (Warner Instruments), digitized at 10 or 20 kHz for the *Shaker* or BK channels, respectively, and stored on a personal computer hard disk. All experiments were carried out at room temperature (22 °C).

Data Analysis. Voltage-activation curves were generated using the measured tail currents and were fitted using Origin (version 5, Microcal Software Inc.) to a two-state Boltzmann equation

$$G/G_{max} \text{ or } I/I_{max} = [1 + e^{-ZF(V-V_{1/2})/RT}]^{-1}$$

where G/G_{max} and I/I_{max} are the normalized conductance and tail current amplitude for the BK and *Shaker* channels, respectively, Z is the activation slope factor, $V_{1/2}$ is the half-activation voltage, and T, F, and R have their usual thermodynamic meaning. Free energy differences between closed (C) and open (O) states of the wild-type or mutant channels were parametrized on the basis of the gating shifts and slopes according to $-ZFV_{1/2}$ ($=-RT\ln[O]/[C]$). Standard errors in $-ZFV_{1/2}$ and $\Delta(ZFV_{1/2})$ [$=-F(Z_{mut}V_{1/2mut} - Z_{wt}V_{1/2wt})$] were calculated by standard linear error propagation.

Recombinant Protein Expression in Xenopus Oocytes. The cRNAs of wild-type or mutant K^+ channels were injected into *Xenopus* oocytes. Protein expression was analyzed 4 days after cRNA injection. Oocytes were first placed in washing buffer containing 20 mM MOPS (pH 7.2), 130 mM NaCl, and 3 mM KCl. Following three rounds of washing, Triton homogenization buffer containing 20 mM Tris-HCl (pH 7.6), 1% Triton X-100, 100 mM NaCl, 1 mM PMSF, 10 mM methionine, and protein inhibitor cocktail (leupeptin, aprotinin, and pepstatin) was added to the oocytes (20 μL per oocyte) followed by vigorous vortexing for 45 s with intermittent cooling on ice. The resultant homogenized solution was centrifuged, and the supernatant containing proteins was removed and analyzed by SDS−PAGE and Western blot analyses, as described below.

Western Blot Analysis. Protein samples were separated by electrophoresis on 7.5% SDS−polyacrylamide gels using standard loading solutions (*14*). The proteins were transferred to nitrocellulose and blocked with 5% BSA, 150 mM NaCl, 20 mM Tris-HCl (pH 7.4), and 0.1% Tween, for 2 h at room temperature. Primary incubation for 1 h with an anti-His tag antibody was followed by washing (4 × 5 min) in blocking solution, and subsequent addition of horseradish peroxidase-conjugated goat anti-mouse secondary antybody (1 h). Immunoblots were developed using the SuperSignal chemi-

luminescence detection system according to directions supplied by the manufacturer (Pierce).

RESULTS

Gating Hinge Mutations in the Shaker K$^+$ Channel. Glycine is unique in its ability to adopt a range of main chain dihedral angles wider than that adopted by other amino acids. In the MthK structure, the inner helix is bent at a glycine residue, and the bend causes the pore to be open. We refer to this position as the glycine gating hinge. It seems reasonable to suppose that conservation of glycine at this position in many different K^+ channels, including voltage-dependent K^+ channels, reflects the requirement for a flexible hinge to open the pore. To test this idea, we made mutant *Shaker* K^+ channels with different amino acids replacing glycine 466, the gating hinge position.

When expressed in *Xenopus* oocytes, wild-type (WT) *Shaker* K^+ channels are closed when the membrane is hyperpolarized and opened upon depolarization (Figure 2A). Eight mutant channels with single-amino acid substitutions at the gating hinge produced no current (Figure 2B). Representative recordings from one example in which the gating hinge glycine was replaced with alanine, the next smallest side chain after glycine, are shown (Figure 2A). Similar results were found in seven additional mutations that were tested (Figure 2B).

One mutant channel with proline at position 466 did yield K^+ currents (Figure 2A,B). A particularly interesting property of the proline mutant is that it not only opened but also was very difficult to close. This reluctance to close can be seen in the voltage dependence of opening: the mutant channel reaches half-maximal activation at around −80 mV, whereas the wild-type channel does not reach half-maximal activation until nearly −25 mV (Figure 2C). In other words, large negative membrane voltages are required to drive the proline mutant channel into a closed conformation. A kinetic manifestation of the shift in equilibrium favoring the opened conformation (in the proline mutant) can be seen in the very slow rate of closure following membrane repolarization (Figure 2A).

That proline's effect is unique among the amino acids substituted at the gating hinge position is not very surprising. Glycine mutated to any other amino acid will tend to reduce flexibility, but proline will tend to produce a rigid artificial kink. We interpret the results presented so far in the following way. The inner helices have to straighten in order to pack against each other at the inner helix bundle to achieve a stable closed conformation of the pore, and they have to bend at the gating hinge in order to open the pore. Eight of nine mutations (Figure 2B) favor a straight helix and thus stabilize the closed conformation, while mutation to proline favors a kinked helix and destabilizes the closed conformation. We do not expect the proline mutant to have a "normal" open pore structure, but we think what is important is the destabilization of a normal closed structure. It is possible that our inability to observe ionic currents for the gating hinge mutants reflects their extremely right-shifted activation profiles which are beyond our measuring capabilities.

Although the conclusion described above, regarding the requirement for flexibility at the gating hinge for the proper opening of the K^+ channel pore, is appealing and makes intuitive sense, another possible explanation for the absence of current when glycine 466 is replaced by other amino acids could be that the mutant channels may not be expressed in

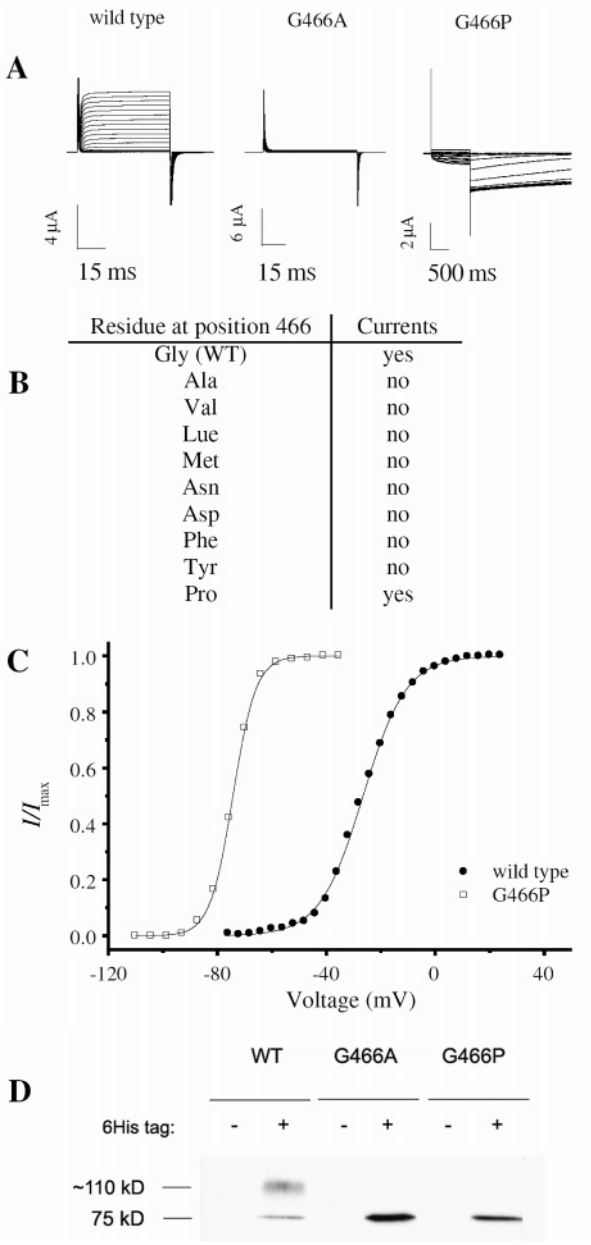

FIGURE 2: Reduced flexibility at the gating hinge of the *Shaker* channel prevents pore opening. (A) K^+ currents recorded from *Xenopus laevis* oocytes under a two-electrode voltage clamp expressing wild-type (WT), G466A, or G466P gating hinge mutant channels. Currents were elicited by various strength depolarizations from holding voltages of −110 mV for the G466P mutant and −85 mV for WT and G466A channels. (B) Effects of replacements at position 466 on K^+ current expression measured as described in panel A. (C) Voltage-activation data for the K^+ channels listed in panel B. Smooth curves correspond to a two-state Boltzmann function (see Data Analysis). The following values were obtained for the activation midpoints and slopes of WT and mutant channels: $V_{1/2,WT} = -26 \pm 0.2$ mV, $Z_{WT} = 3.2 \pm 0.1$, $V_{1/2,G466P} = -74 \pm 0.1$ mV, and $Z_{G466P} = 6.0 \pm 0.2$. (D) Functional expression of the G466A and G466P K^+ channel mutants in *Xenopus* oocytes. Immunoblots are from membrane proteins extracted from *Xenopus* oocytes expressing the indicated native (−) or six-His-tagged (+) *Shaker* channel constructs. Markers to the left correspond to the mature fully glycosylated (110 kDa) and partially glycosylated (75 kDa) *Shaker* protein bands (*15*, *16*).

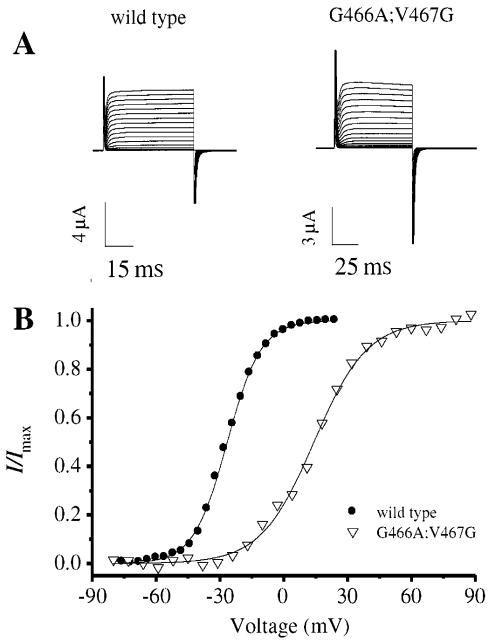

FIGURE 3: Pore opening is recovered in a double mutant lacking the natural gating hinge but containing an artificial adjacent one. (A) K^+ currents recorded from *X. laevis* oocytes under a two-electrode voltage clamp expressing the wild-type (WT) or G466A/V467G gating hinge double mutant channel. Currents were elicited by various strength depolarizations from holding voltages of −85 mV followed by repolarization to the holding potential. (B) Voltage-activation data for the K^+ channels given in panel A. Smooth curves correspond to a two-state Boltzmann function (see Experimental Procedures). The following values were obtained for the activation midpoint and slope of the G466A/V467G mutant channel: $V_{1/2} = 14 \pm 0.1$ mV and $Z = 2.0 \pm 0.1$.

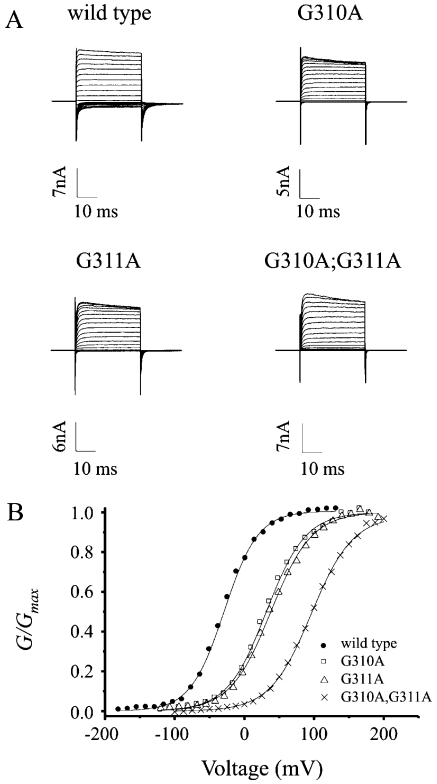

FIGURE 4: Pore opening of the BK channel is more difficult in gating hinge mutants with reduced flexibility. (A) K^+ current families recorded from inside-out patches expressing the G310A or G311A single mutant channel or the corresponding double mutant (see Experimental Procedures). Currents were elicited by voltage steps between −100 and 200 mV and were recorded in the presence of 100 μM Ca^{2+} in the bath, conditions at which the maximal open probability has been reached for all mutant channels (not shown). Tail potentials are −60 mV. (B) $G-V$ relations for the K^+ channels given in panel A. Smooth curves correspond to a two-state Boltzmann function (see Experimental Procedures). The following values were obtained for the activation midpoints and slopes of the single and double mutant channels: $V_{1/2,WT} = -29.0 \pm 0.7$ mV, $Z_{WT} = 1.00 \pm 0.03$, $V_{1/2,G310A} = 31.0 \pm 1.0$ mV, $Z_{G310A} = 0.90 \pm 0.03$, $V_{1/2,G311A} = 37.9 \pm 1.0$ mV, $Z_{G311A} = 0.86 \pm 0.02$, $V_{1/2,G310A/G311A} = 97.6 \pm 0.6$ mV, and $Z_{G310A/G311A} = 0.82 \pm 0.02$.

oocytes or for some reason may never have reached the membrane. To address this latter possibility, we have measured protein expression levels of the wild-type, G466A, and G466P channel proteins in oocytes. As could be seen from the Western blot analysis of Triton-extracted oocyte proteins (Figure 2D), the G466A nonconducting mutant and, as expected, the G466P functional mutant are both expressed in oocytes, although they migrate at a position corresponding to the partially glycosylated *Shaker* form [Figure 2D (*15*, *16*)]. This evidence can still not be fully conclusive with regard to the cell surface localization of the G466A mutant; however, further evidence in support of normal cell surface expression of this mutant will be presented below.

If the absence of ionic currents in the majority of gating hinge mutants results from an inability to bend the inner helices, then it should be possible to introduce a secondary hinge point that will suppress the effect of mutating the normal gating hinge. This is indeed the case (Figure 3). In the background of a glycine 466 alanine mutant channel, which by itself does not produce K^+ currents in oocytes (Figure 2A), a second mutation of valine 467 to glycine has a rescuing influence. The double mutant channel requires more positive membrane voltages than the wild-type channel to open, but there is no reason to expect wild-type gating properties since the hinge point has been moved along the helix. The main point of this experiment is that it provides very strong evidence for the importance of a flexible hinge point in the inner helix to open the channel. Furthermore, recovery of current by a secondary mutation argues that the primary mutation prevented opening, not channel misfolding or nonmature targeting. The results presented here for the gating hinge mutants of the *Shaker* channel (studied in the ooctye expression system) are similar to results obtained in the mammalian expression system (R. Horn, personal communication).

Gating Hinge Mutations in the BK Channel. BK channels are K^+ channels gated by intracellular Ca^{2+} concentration and membrane voltage (*17*, *18*). In a BK channel from *Homo sapiens* (hBK), the gating hinge position corresponds to glycine 311. An unusual feature of this channel is that it has a second glycine at an adjacent position, 310 (Figure 1). We studied the effect of mutating each of these glycine residues to alanine, one at a time and together; the results are shown in Figure 4. Voltage-dependent activation was studied in inside-out membrane patches excised from *Xenopus* oocytes at a fixed concentration of bath Ca^{2+} (see Experimental Procedures). Both the single glycine mutant channels and the corresponding double mutant channel express K^+ currents (Figure 4A). Either single mutation shifted the midpoint of the voltage-activation curve to positive membrane voltages by a roughly equal amount, and the double mutation caused twice the voltage shift (∼130 mV). In contrast to the *Shaker*

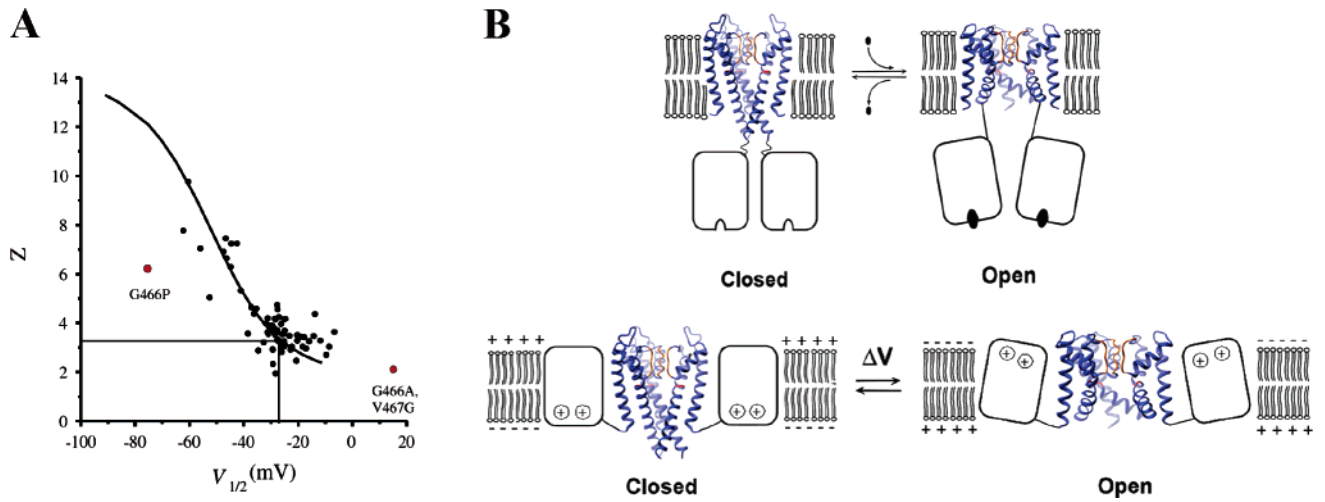

FIGURE 5: Flexibility at the gating hinge position is essential for pore opening in both ligand- and voltage-dependent K^+ channels. (A) The Z and $V_{1/2}$ phenomenological gating parameter values of the G466P and G466A/V467G single and double mutant channels, respectively, mapped onto the $Z-V_{1/2}$ phase space (red circles) in the context of a previously observed experimental correlation between the Z and $V_{1/2}$ values of wild-type and mutant *Shaker* channel proteins (black circles). Straight lines are for the wild-type *Shaker* channel values (refer to ref *11* for further details). (B) Gating mechanics involving gating hinge motions is conserved in both ligand-gated and voltage-dependent K^+ channels.

K^+ channel, the hBK channel still opened without a glycine gating hinge, but the equilibrium was shifted significantly toward the closed state. When parametrized in terms of gating shifts and slopes using a simple two-state Boltzmann isotherm (*11*), the equilibrium for the pore opening transition is shifted by more than 3 kcal/mol toward closed, reflecting the fact that it is a 100-fold more difficult to open the pore of the gating hinge-deficient hBK channel than that of the wild-type channel. As in the case of the *Shaker* K^+ channel, substitution of glycine 311, the primary gating hinge, with proline (G311P mutant) resulted in a channel for which the midpoint activation voltage ($V_{1/2}$) is shifted to the left along the voltage axis by more than 30 mV as compared to that of the wild-type channel (not shown), a manifestation of an open state stabilization effect. The results presented here for the BK channel are thus consistent with the results obtained for the *Shaker* K^+ channel.

DISCUSSION

In this study, we ask whether voltage-dependent K^+ channels gate their pore by bending their inner helices at a glycine gating hinge. The crystal structure of the opened MthK K^+ channel showed such a bent hinge in the inner helix compared to the straight inner helix in the closed KcsA K^+ channel structure (*9*). Conservation of a glycine amino acid at the corresponding position in most K^+ channels led to the proposal of a conserved pore-opening mechanics, independent of the stimulus leading to opening. The experiments presented here are very simple and direct; they address the outcome of mutations at or near the proposed gating hinge position in two different voltage-dependent K^+ channels, *Shaker* and hBK. The effects of mutations are not identical in the two channels, but they are similar and underscore the importance of having a glycine residue at the gating hinge. It seems that the ability to bend the inner helix (favored by the conformational flexibility conferred by glycine) is important for channel opening, while the ability to straighten the inner helix (hindered by proline) seems to be important for proper closure of the pore.

The important weight given here to the results on the *Shaker* gating hinge mutations, specifically the G466P mutant that locks the channel open and the gating hinge recovery double mutant G466A/V467G that stabilizes the closed state of the channel, may raise some reservations as, after all, as shown by other labs, many mutations along the S6 inner helix are gating sensitive, showing similar right or left shifting effects of the activation curves upon mutation. It is interesting to note, however, that the Z and $V_{1/2}$ values of the G466P and G466A/V467G mutants (see the legends of Figures 2 and 3), when mapped on the $Z-V_{1/2}$ phase space, lie significantly out of the experimental correlation observed between the Z and $V_{1/2}$ values of many wild-type and *Shaker* channel variants (Figure 5A) (*11*). This finding, so rarely observed for the many *Shaker* mutations that have been characterized, even for cases in which *Shaker* positions are replaced with alanines, tryptophans, lysines, aspartates, or asparagines, further highlights the importance of the gating hinge position to the mechanics of pore opening in this channel. Mutations at the hinge position, if functional, result in channels with a modified gating pathway; that is, such channels no longer conform to the detailed gating model describing the wild type channel (the mutation of which normally affects only the ratio of equilibrium constants connecting the model states but not the gating model itself). Rather, a different gating model needed to be invoked to explain such outlier channel behavior which probably reflects the perturbed pore structure of the channel upon mutations at the gating hinge.

The results on the *Shaker* K^+ channel presented here highlight the importance of the gating hinge for the mechanics of pore opening; however, they shed no light on how wide the open pore conformation of the *Shaker* K^+ channel is as compared to the MthK structure. Recent data published by Yellen and colleagues (*19*) argue that the open pore diameter at the region of the bundle crossing is narrower for the *Shaker* channel than what is revealed by the MthK open channel structure. The conclusion reached in that study that, in the open state, the inner pore helices of the *Shaker*

channel maintain a KcsA-like bundle crossing motif (*19*) is somewhat inconsistent with the results presented here. This study attributes an important role in pore opening to the PVP hinge point, a sequence motif conserved in all voltage-gated K^+ channels located at the intracellular bottom part of the inner helices, and minimizes the role played by the conserved glycine gating hinge as found here. As already suggested (*19*), it is possible that pore opening mechanics of the *Shaker* channel is brought about by concerted or sequential motions (yet to be determined) along both hinge points. The type and magnitude of motions along both hinge points might explain differences in open pore conformations expected for different subtypes of voltage-gated K^+ channels. We think, however, that the glycine gating hinge is universal to all K^+ channels (see Figure 1) and maybe to other ion channels, and that other slight adaptations (like the PVP motif of the *Shaker* channel) accumulated during evolution to accommodate variations in conductance and gating mechanisms among different channels.

The interpretation of the essential role of the glycine gating hinge in pore opening is further strengthened by a comprehensive sequence−function analysis of the K^+ channel family using evolutionary information (*20*) and by functional studies of gating in both G-protein-dependent (GIRK) K^+ and Na^+ channels. Specifically, in the GIRK K^+ channel, introduction of a proline into the inner helix gating hinge led to a constitutively activated K^+ channel (*21*, *22*). In the bacterial sodium channel NaChBac, mutation of the glycine gating hinge (position 219) to proline, which would strongly favor bending of the α-helix, greatly enhances activation by shifting its voltage dependence to the left along the voltage axis by 51 mV and slowing deactivation by 2000-fold (*23*). Thus, inner helix motions allowed by the glycine gating hinge appear to underlie gating in a wide range of K^+ channels (Figure 5B) and perhaps in other related channels. Upon changes in chemical or electrical potential, gating domains of K^+ channels exert a lateral force on the C-terminal extent of the inner helices, causing the gating hinge to bend, the bundle to come apart, and the pore to open.

REFERENCES

1. Zagotta, W. N., Hoshi, T., and Aldrich, R. W. (1994) *Shaker* potassium channel gating III: evaluation of kinetic models for activation, *J. Gen. Physiol. 103*, 321−362.
2. Sigworth, F. J. (1994) Voltage gating of ion channels, *Q. Rev. Biophys. 27*, 1−40.
3. Yellen, G. (1998) The moving parts of voltage-gated ion channels, *Q. Rev. Biophys. 31*, 239−295.
4. Bezanilla, F. (2000) The voltage sensor in voltage-dependent ion channels, *Physiol. Rev. 80*, 555−592.
5. Yi, B. A., Minor, D. L., Jr., Lin, Y. F., Jan, Y. N., and Jan, L. Y. (2001) Controlling potassium channel activities: Interplay between the membrane and intracellular factors, *Proc. Natl. Acad. Sci. U.S.A. 98*, 11016−11023.
6. Hille, B. (2001) *Ion Channels of Excitable Membranes*, Sinauer Associates, Sunderland, MA.
7. Doyle, D. A., Morais Cabral, J. H., Pfuetzner, R. A., Kuo, A., Gulbis, J. M., Cohen, S. L., Chait, B. T., and MacKinnon, R. (1998) The structure of the potassium channel: molecular basis of K^+ conduction and selectivity, *Science 280*, 69−77.
8. Zhou, Y., Morais-Cabral, J. H., Kaufman, A., and MacKinnon, R. (2001) Chemistry of ion coordination and hydration revealed by a K^+ channel: Fab complex at 2.0 Å resolution, *Nature 414*, 43−48.
9. Jiang, Y., Lee, A., Chen, J., Cadene, M., Chait, B. T., and MacKinnon, R. (2002) The open pore conformation of potassium channels, *Nature 417*, 523−526.
10. Jiang, Y., Lee, A., Chen, J., Cadene, M., Chait, B. T., and MacKinnon, R. (2002) Crystal structure and mechanism of a calcium-gated potassium channel, *Nature 417*, 515−522.
11. Yifrach, O., and MacKinnon, R. (2002) Energetics of pore opening in a voltage-gated K^+ channel, *Cell 111*, 231−239.
12. Fleishman, S. J., Yifrach, O., and Ben-Tal, N. (2004) An evolutionarily conserved network of amino acids mediates gating in voltage-dependent potassium channels, *J. Mol. Biol. 340*, 307−318.
13. Hoshi, T., Zagotta, W. N., and Aldrich, R. W. (1990) Biophysical and molecular mechanisms of *Shaker* potassium channel inactivation, *Science 250*, 533−538.
14. Laemmli, U. K. (1970) Cleavage of structural proteins during the assembly of the head of bacteriophage T4, *Nature 227*, 680−685.
15. Santacruz-Toloza, L., Huang, Y., John, S. A., and Papazian, D. M. (1994) Glycosylation of *Shaker* potassium channel protein in insect cell culture and in *Xenopus* oocytes, *Biochemistry 33*, 5607−5613.
16. Kobertz, W. R., Williams, C., and Miller, C. (2000) Hanging gondola structure of the T1 domain in a voltage-gated K^+ channel, *Biochemistry 39*, 10347−10352.
17. Calderone, V. (2002) Large-conductance, Ca^{2+}-activated K^+ channels: function, pharmacology and drugs, *Curr. Med. Chem. 9*, 1385−1395.
18. Magleby, K. L. (2003) Gating mechanism of BK (Slo1) channels: so near, yet so far, *J. Gen. Physiol. 121*, 81−96.
19. Webster, S. M., Del Camino, D., Dekker, J. P., and Yellen, G. (2004) Intracellular gate opening in *Shaker* K^+ channels defined by high-affinity metal bridges, *Nature 428*, 864−868.
20. Shealy, R. T., Murphy, A. D., Ramarathnam, R., Jakobsson, E., and Subramaniam, S. (2003) Sequence-function analysis of the K^+-selective family of ion channels using a comprehensive alignment and the KcsA channel structure, *Biophys. J. 84*, 2929−2942.
21. Sadja, R., Smadja, K., Alagem, N., and Reuveny, E. (2001) Coupling G $\beta\gamma$-dependent activation to channel opening via pore elements in inwardly rectifying potassium channels, *Neuron 29*, 669−680.
22. Jin, T., Peng, L., Mirshahi, T., Rohacs, T., Chan, K. W., Sanchez, R., and Logothetis, D. E. (2002) The $\beta\gamma$ subunits of G proteins gate at K^+ channel by pivoted bending of a transmembrane segment, *Mol. Cell 10*, 469−481.
23. Zhao, Y., Yarov-Yarovoy, V., Scheuer, T., and Catterall, W. A. (2004) A gating hinge in Na^+ channels; a molecular switch for electrical signaling, *Neuron 41*, 859−865.

BI048377V